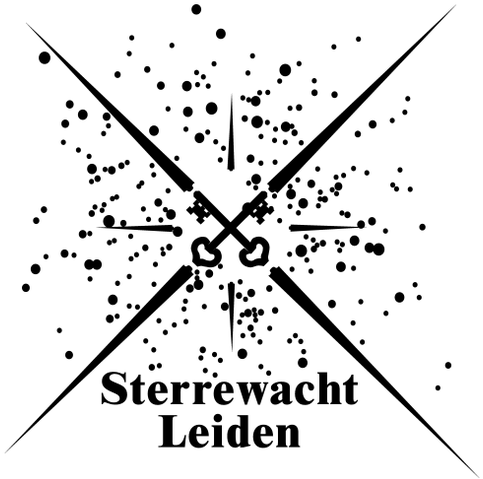

A model of electronically-excited states of N_2 and its extreme-ultraviolet spectrum

A.N. HEAYS
Leiden University, The Netherlands

B.R. LEWIS and S.T. GIBSON
Research School of Physics and Engineering,
The Australian National University

Motivation

- N_2 is abundant in several UV environments: Earth, Titan, interstellar clouds, protoplanetary systems.

- XUV absorption leads to dissociation - a source of N atoms in ongoing chemistry.

- The spectrum consists of predissociating resonances and must be treated at full complexity in a structured radiation field.

The electronic spectrum

(by electron energy loss)

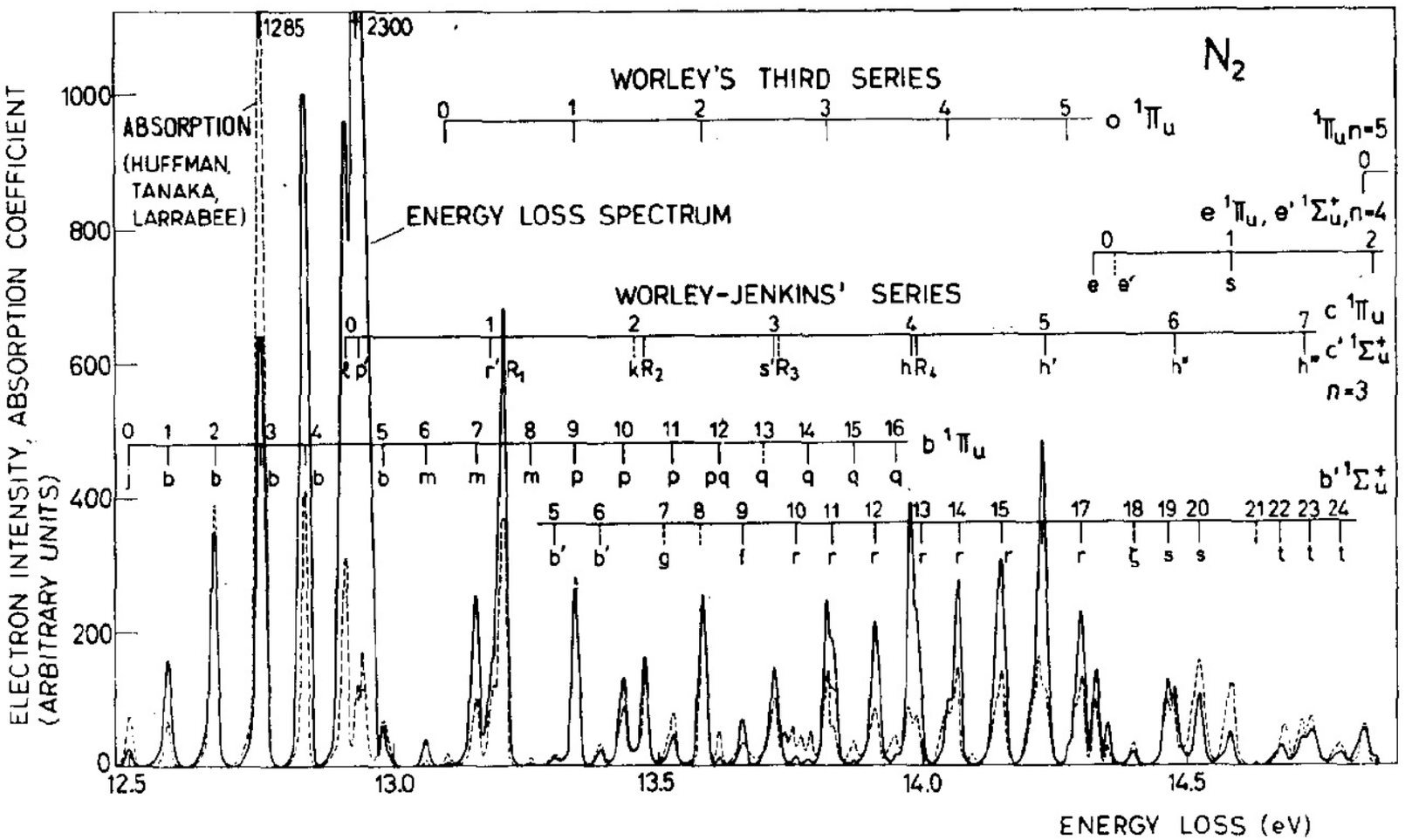

Geiger & Schroeder (1969), *J. Chem. Phys.* 50:7

Rydberg-valence interactions distort the vibrational band structure.

Rotational structure in $^{14}N^{15}N$

(DESIRs FTS at synchrotron SOLEIL)

$$^{14}\mathrm{N}^{15}\mathrm{N}\ b\,^1\Pi_u\,(v'=5) \leftarrow X\,^1\Sigma_g^+(v''=0)$$

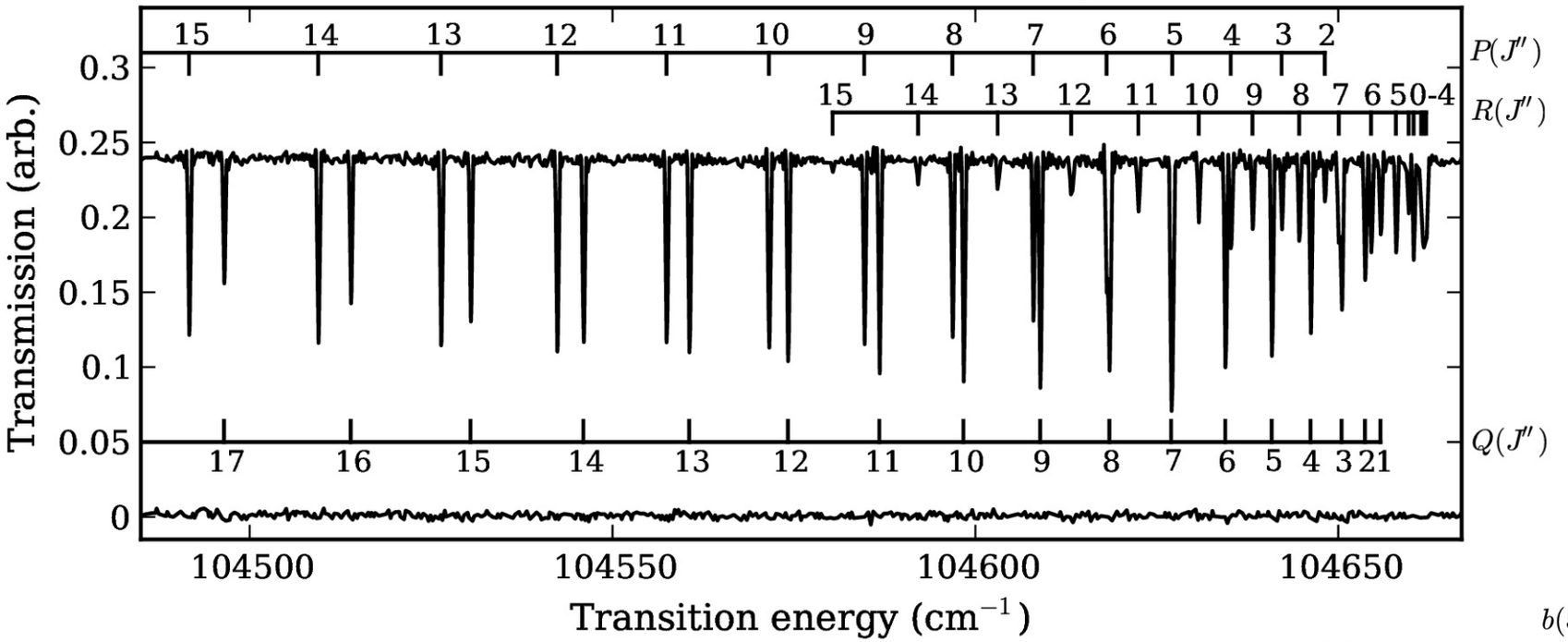

Patterns of line energies and strengths are perturbed homogeneously and heterogeneously.

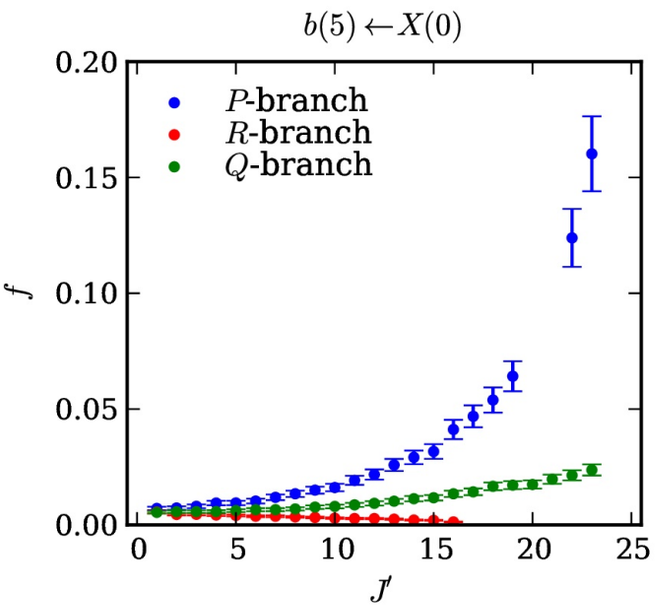

Rotationally dependent accidental predissociation

$$^{14}\mathrm{N}^{15}\mathrm{N}\ c_3\,{}^1\Pi_u\,(v'=2) \leftarrow X\,{}^1\Sigma_g^+(v''=0)$$

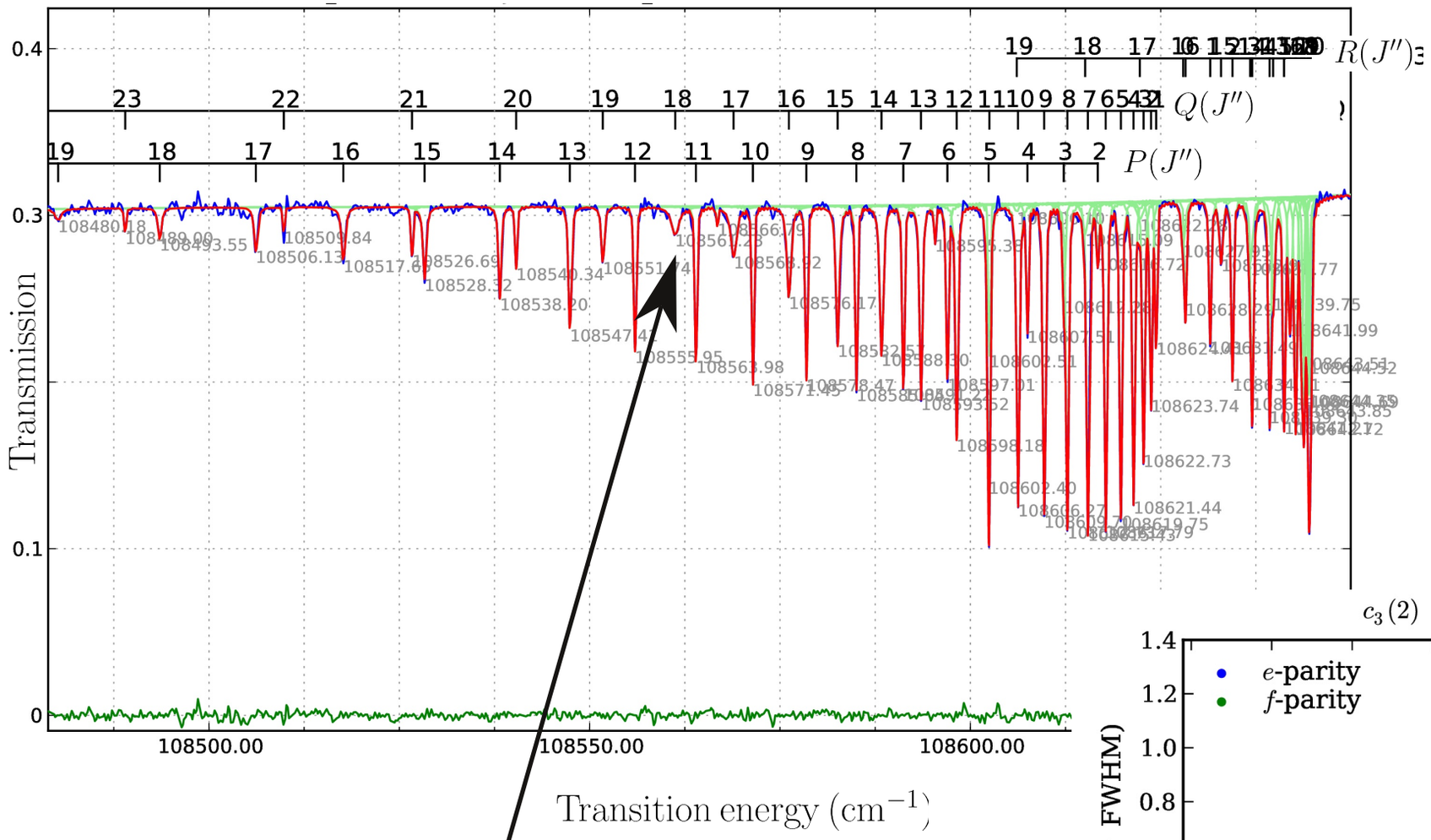

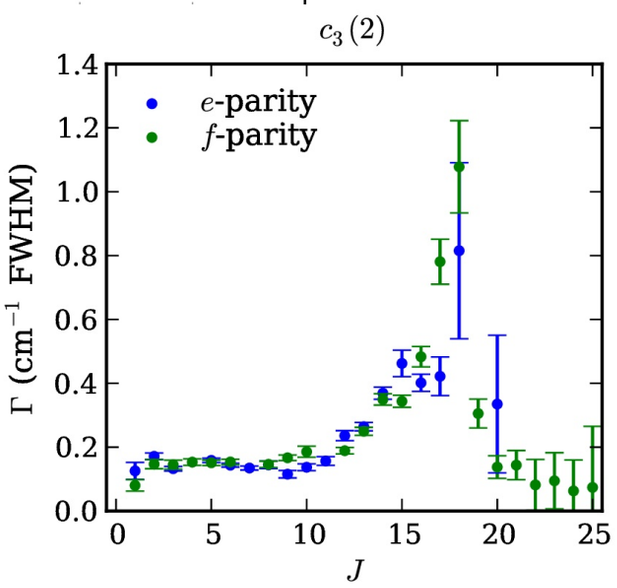

Line broadening peaks at J=18.

The coupled Schrödinger equation

$$\psi_i(\mathbf{r}, R) = \begin{cases} \chi_i(R) \cdot \phi_i(\mathbf{r}; R), & \text{Born-Oppenheimer} \\ \sum_j \chi_{ij}(R) \cdot \phi_j(\mathbf{r}; R), & \text{coupled} \end{cases}$$

$$\boldsymbol{\chi}(R) = \begin{pmatrix} \chi_{11}(R) & \chi_{12}(R) & \chi_{13}(R) \\ \chi_{21}(R) & \chi_{22}(R) & \\ \chi_{31}(R) & & \ddots \end{pmatrix}, \quad \mathbf{V}(R) = \begin{pmatrix} V_1(R) & \langle \phi_1 | H^{\mathrm{el}} | \phi_2 \rangle & \\ \langle \phi_2 | H^{\mathrm{el}} | \phi_1 \rangle & V_2(R) & \\ & & \ddots \end{pmatrix}$$

$$\frac{d^2}{dR^2}\boldsymbol{\chi}(R) = \frac{-2\mu}{\hbar^2}\boldsymbol{\chi}(R)\Big[E - \mathbf{V}(R)\Big] - \boldsymbol{\chi}(R)\frac{l(l+1)}{R^2}$$

- Potential energy curves and off-diagonal coupling terms are optimised with reference to experiment.

- The radial Schrödinger is solved explicitly.

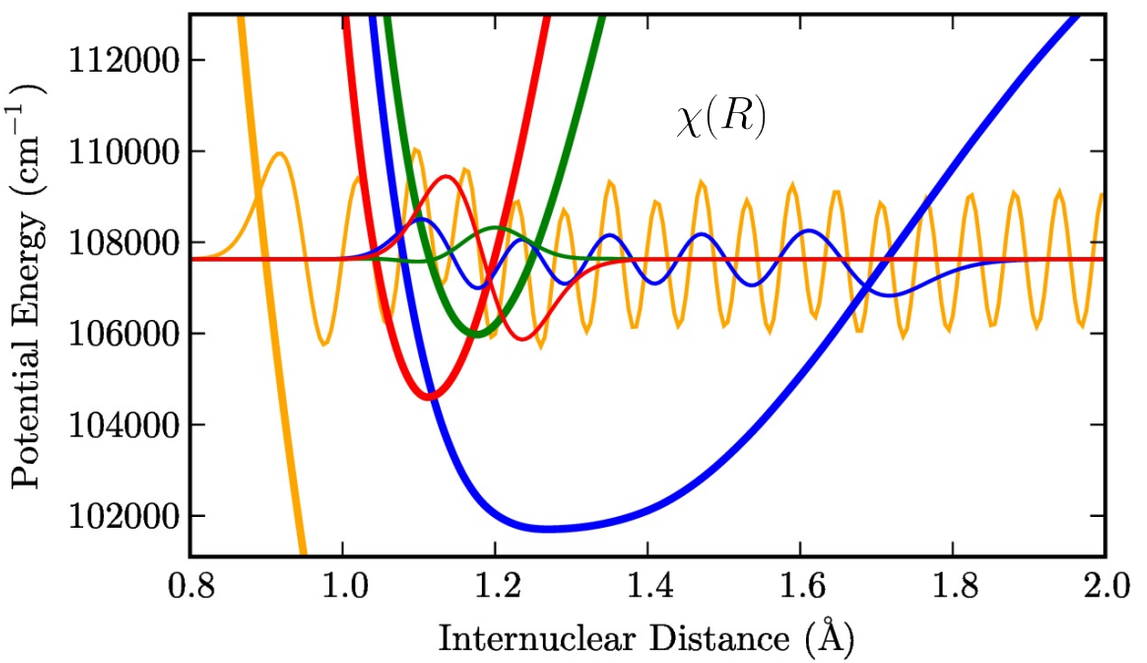

The theoretical picture of excited states

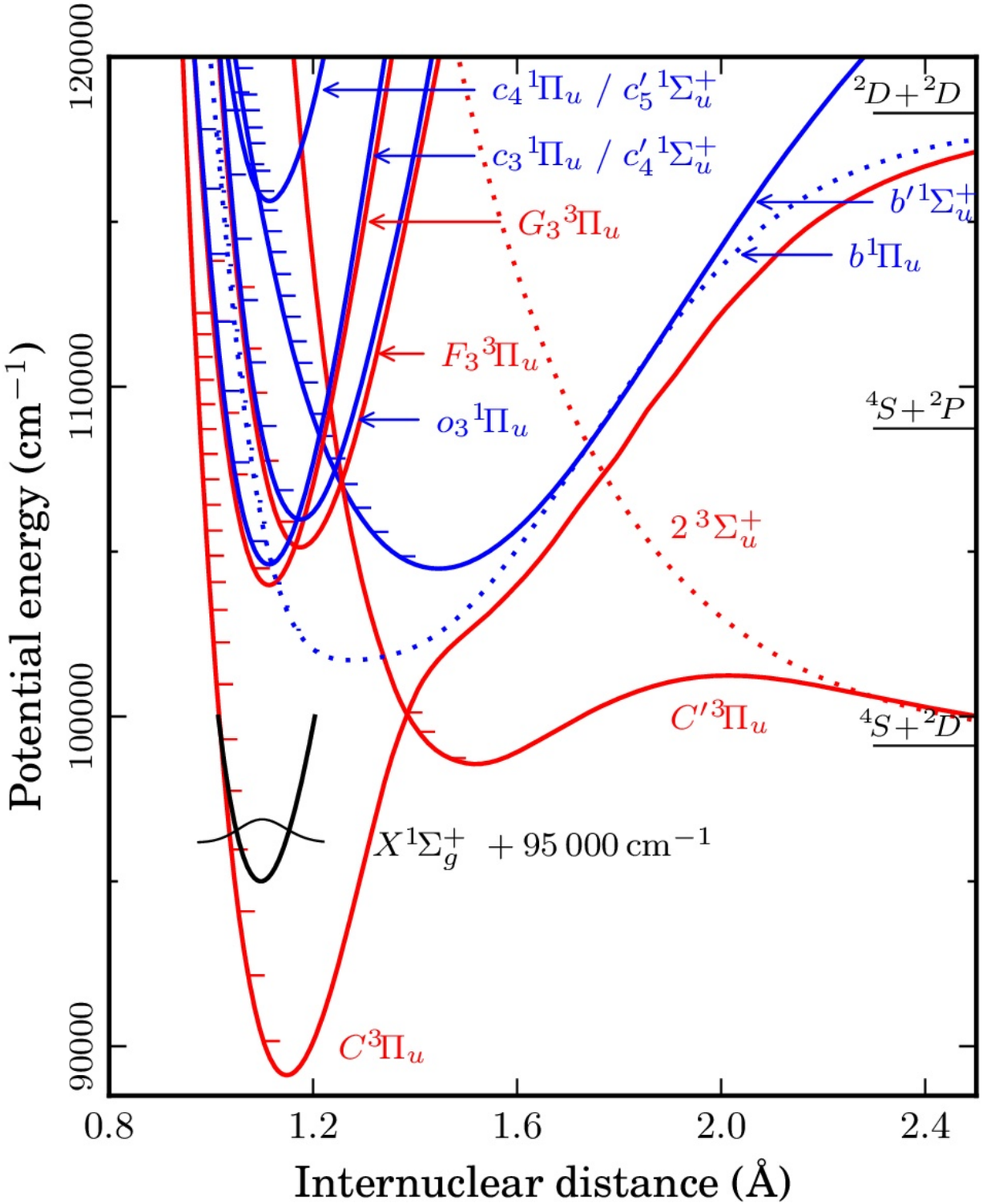

- All $^1\Pi$ and $^1\Sigma^+$ states appear in photoabsorption spectra from the ground state.

- Dissociation below 117,500cm-1 occurs because of spin-orbit interactions with $^3\Pi$ and $^3\Sigma^+$states.

The experimental database

- Classical light source absorption/emission and photographic plates.
- Synchrotron radiation and photoelectric detection.
- Laser based experiments.
- Electron excitation.

Mostly at room temperature, mostly $^{14}N_2$, and with varying experimental accuracies / precision / systematic uncertainties.

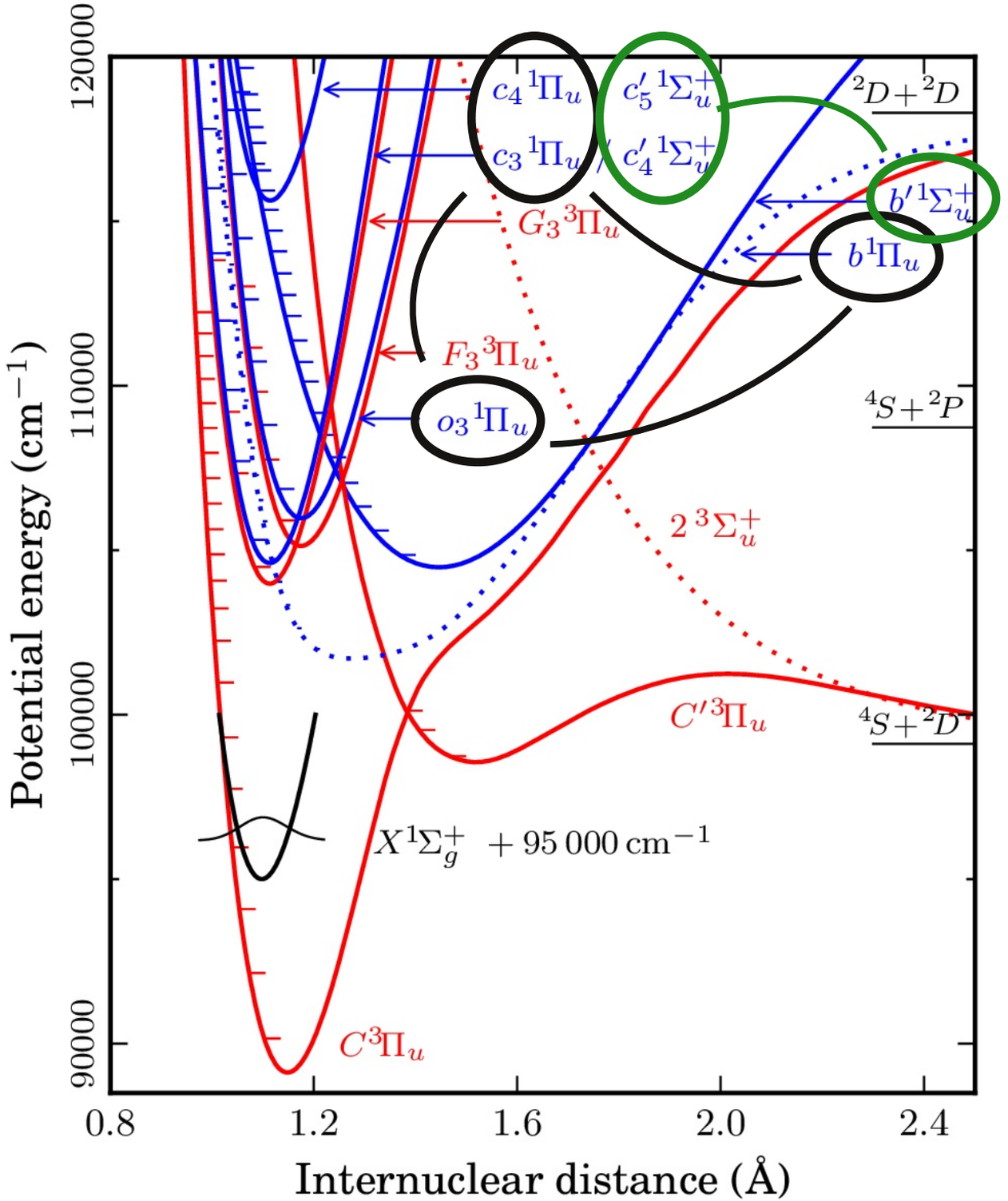

Homogeneous electronic coupling.

$$^1\Pi_u \sim {}^1\Pi_u$$
$$^1\Sigma_u^+ \sim {}^1\Sigma_u^+$$
$$^3\Pi_u \sim {}^3\Pi_u$$

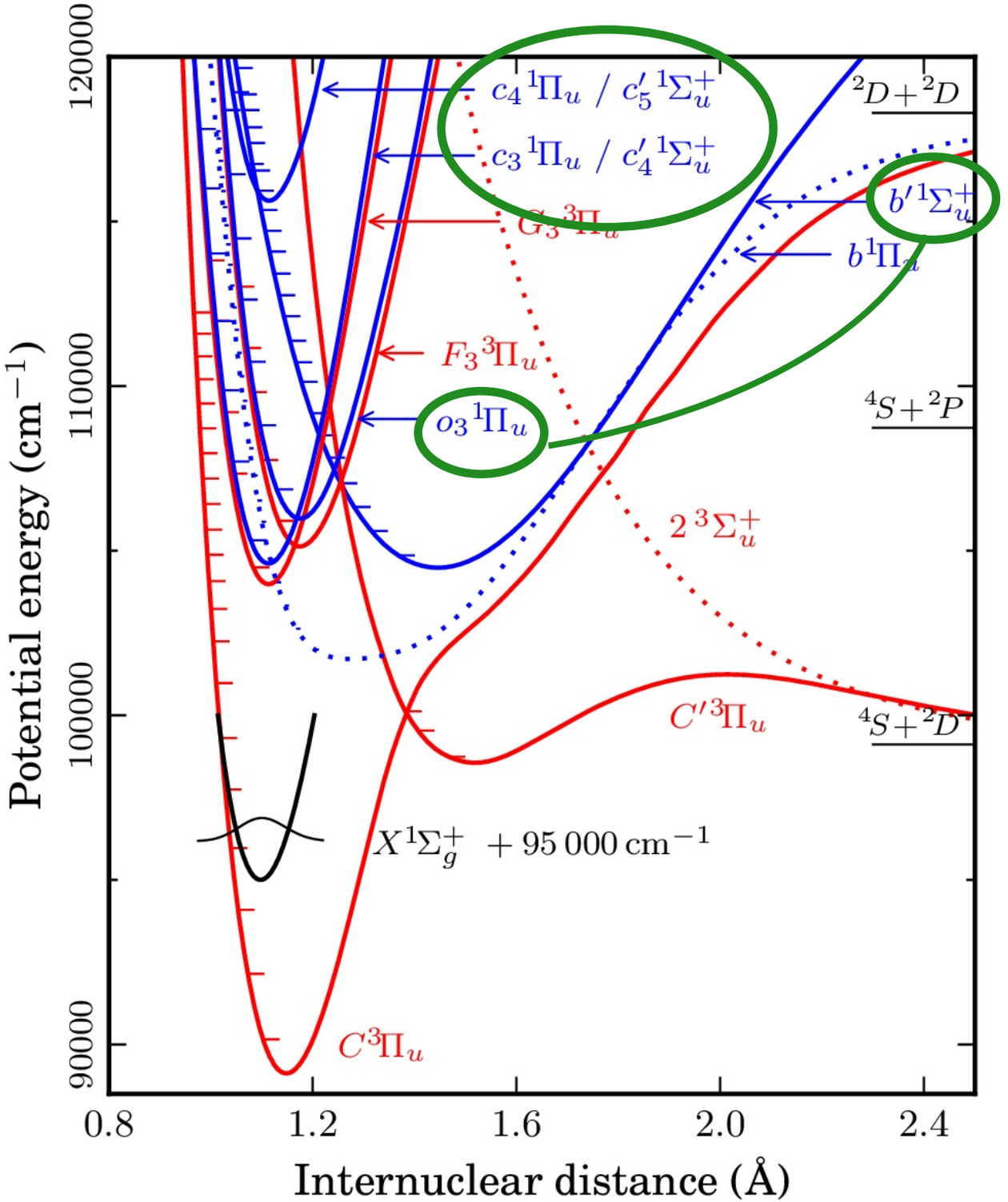

Heterogeneous rotational coupling.

$$^1\Pi_u \sim {}^1\Sigma_u^+$$

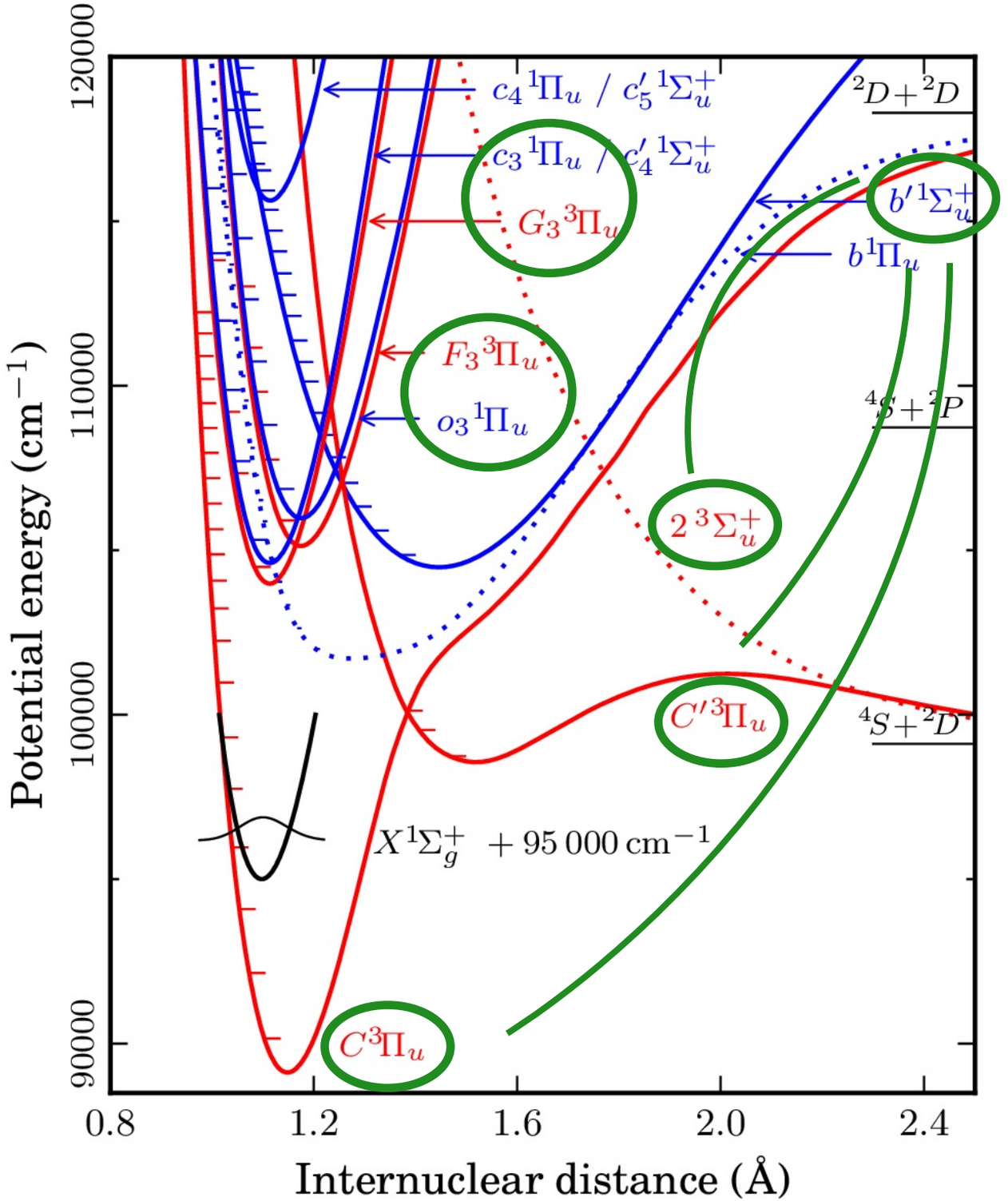

Spin-orbit coupling.

$$^1\Pi_u \sim {}^3\Pi_u$$
$$^1\Pi_u \sim {}^3\Sigma_u^+$$
$$^1\Sigma_u^+ \sim {}^3\Pi_u$$

To be done.

Simulated spectra

- Comparison with SOLEIL FTS high resolution spectra.

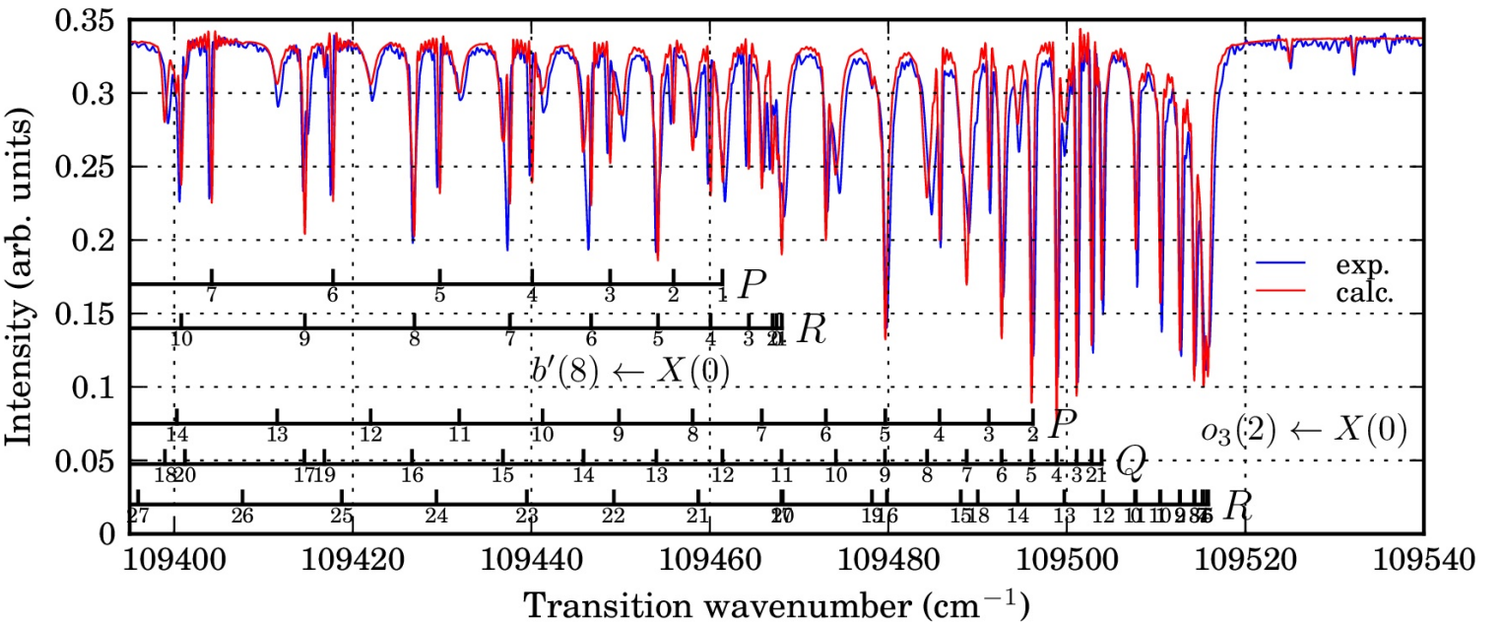

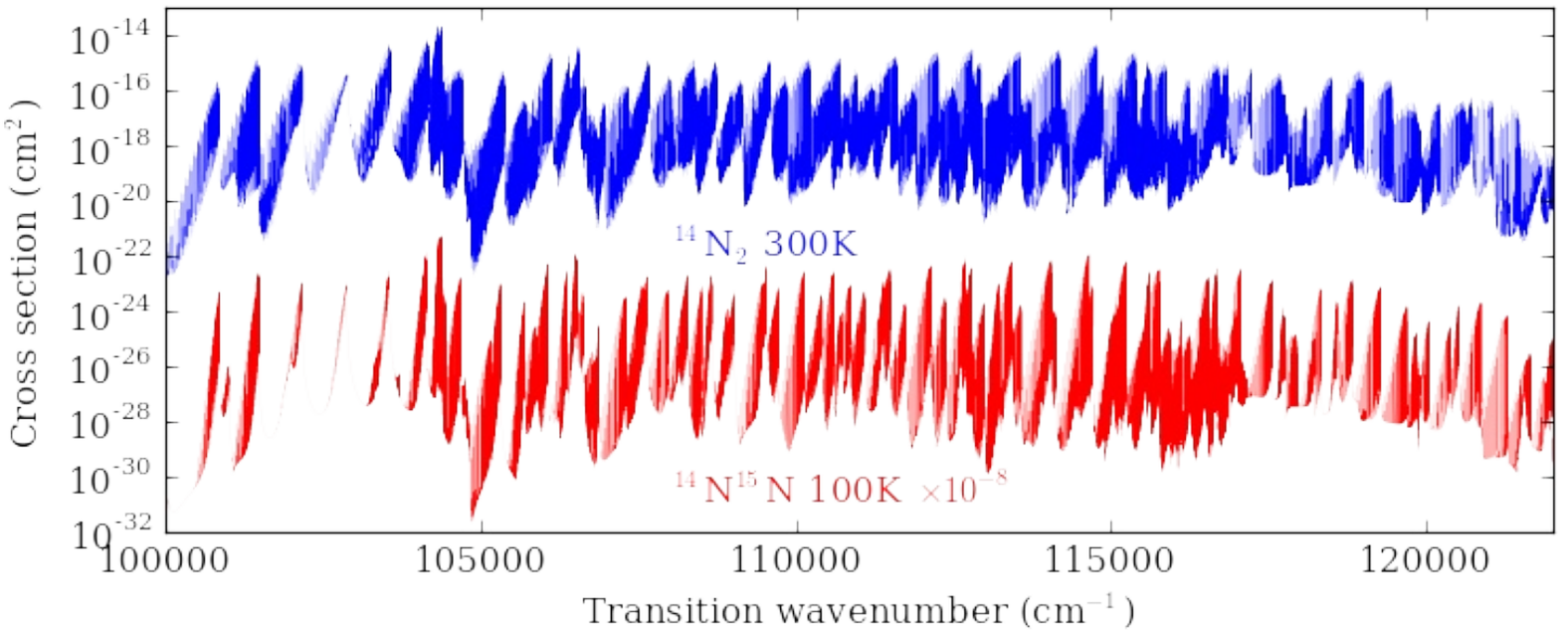

- Extrapolation to other isotopologues and temperatures

The effect of quantum interference on absorption intensities

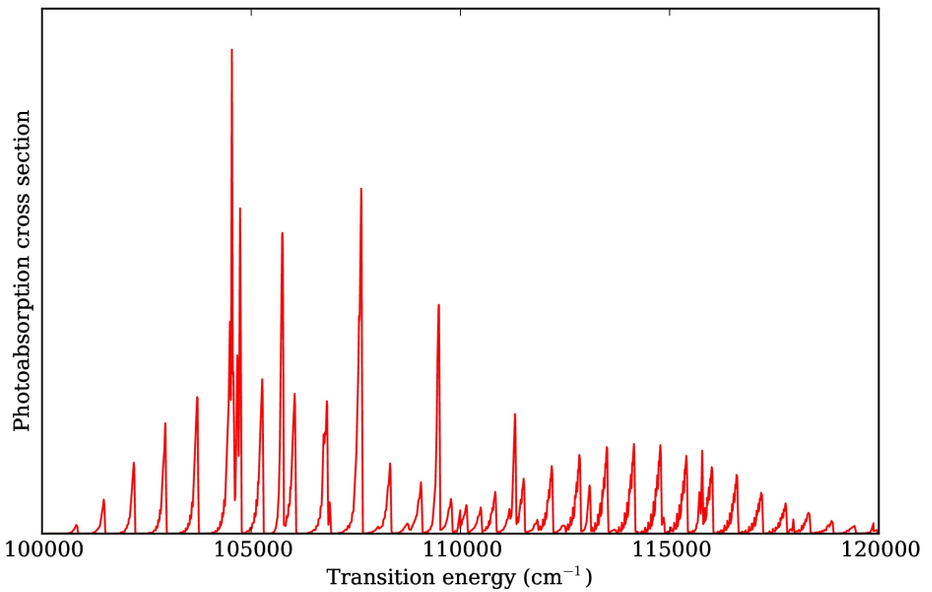

Uncoupled diabatic model with Franck-Condon transition strengths.

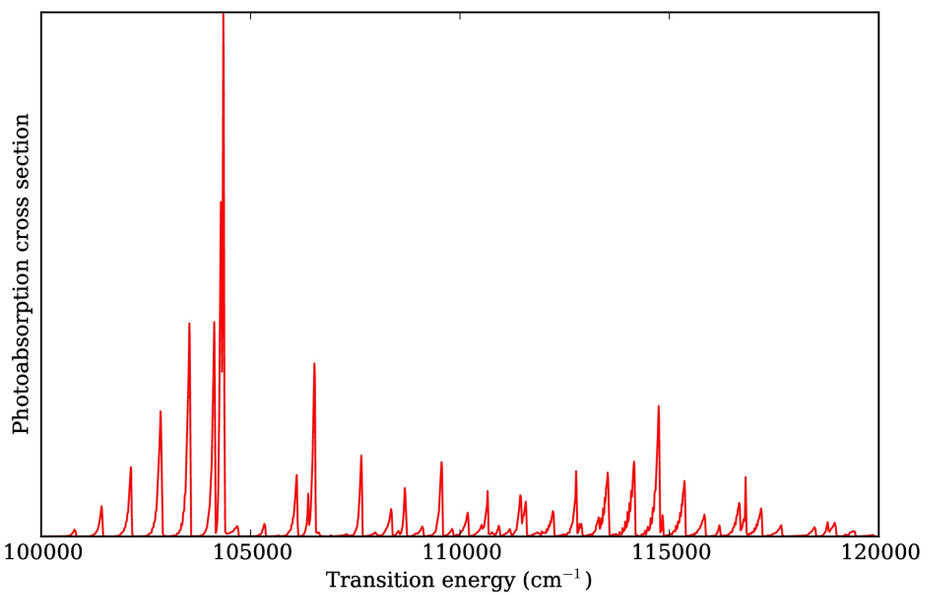

Coupled model.

Level crossings of b' $^1\Sigma_u^+$ and $o_3\,^1\Pi_u$

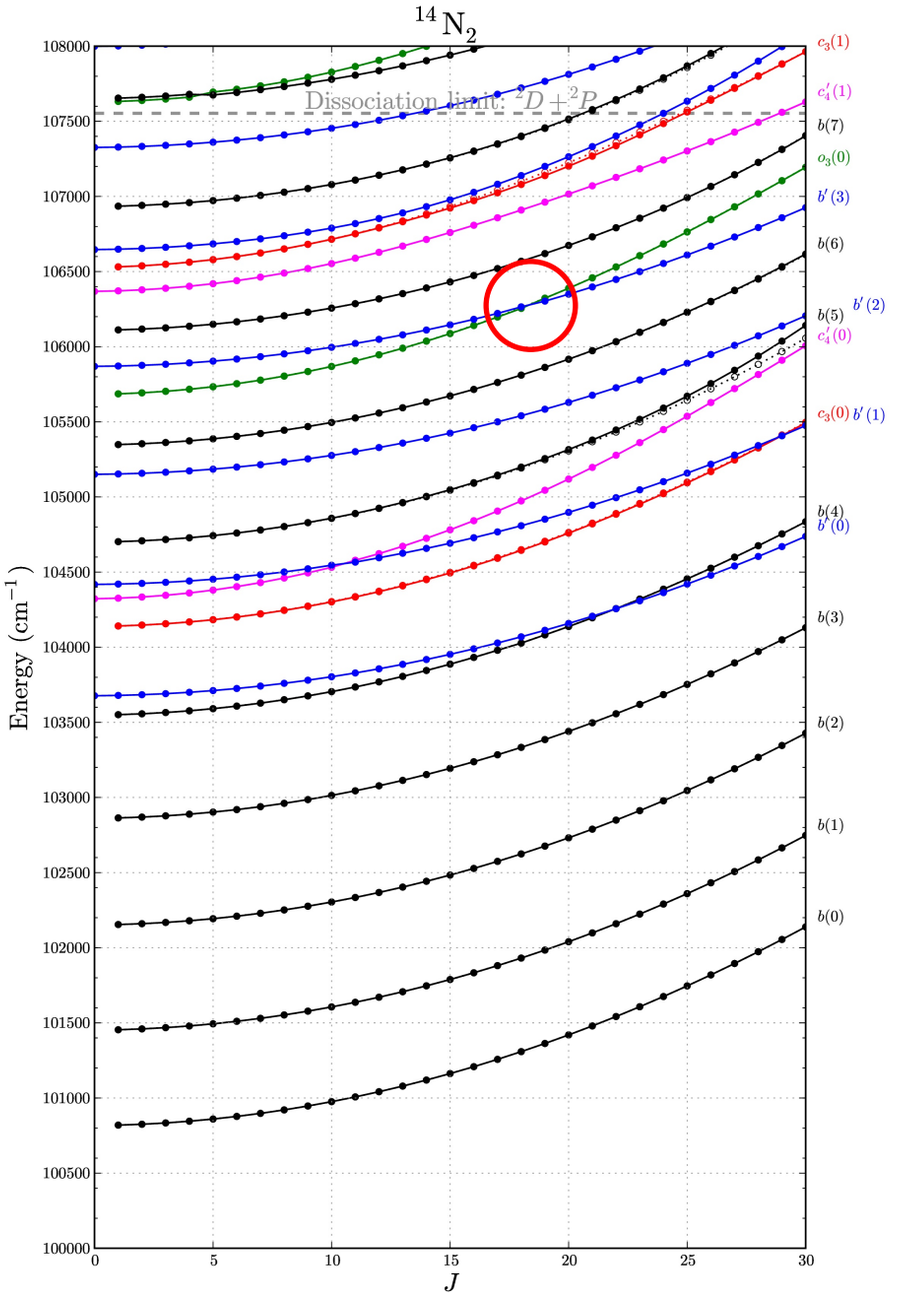

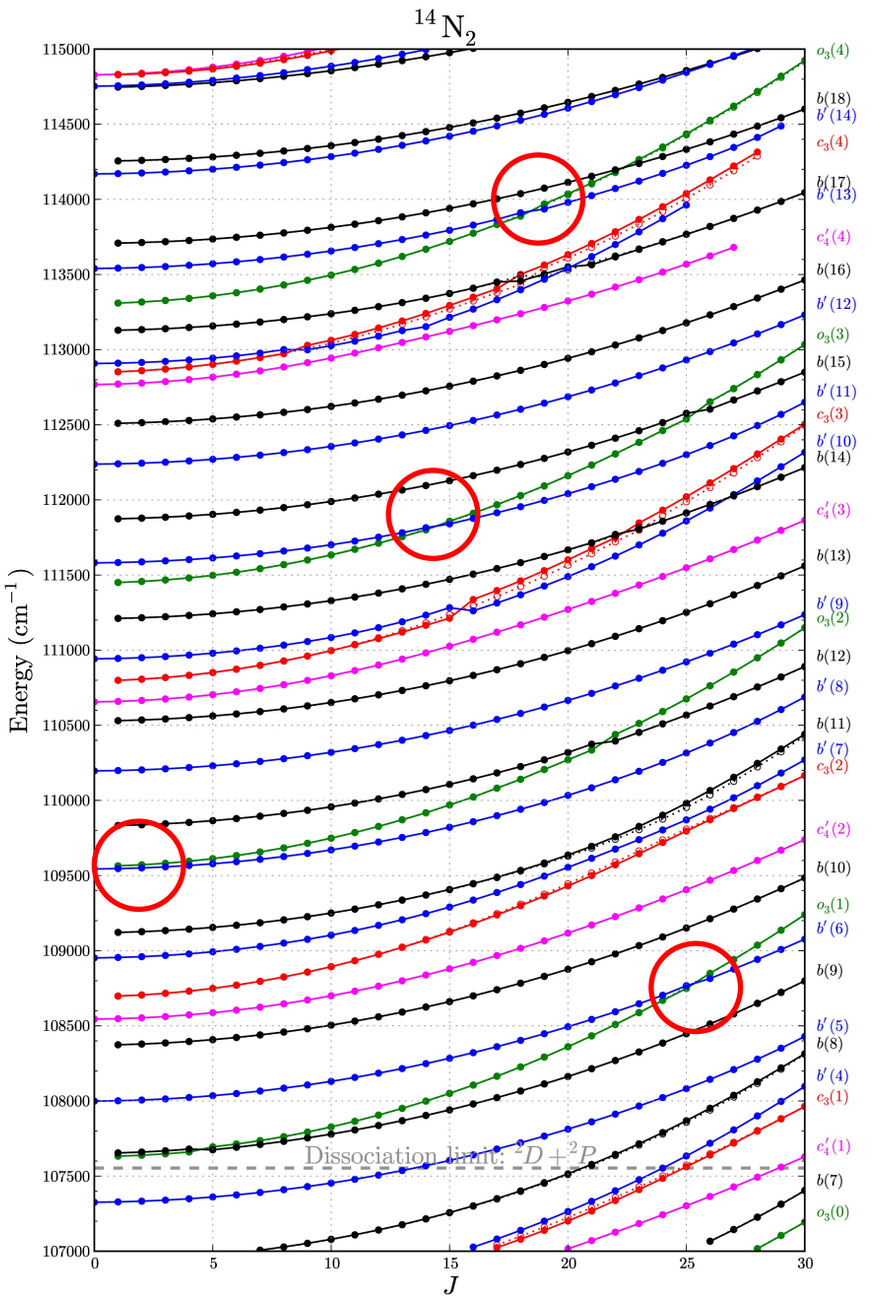

Rotational interaction of b' $^1\Sigma_u^+$ and o$_3$ $^1\Pi_u$

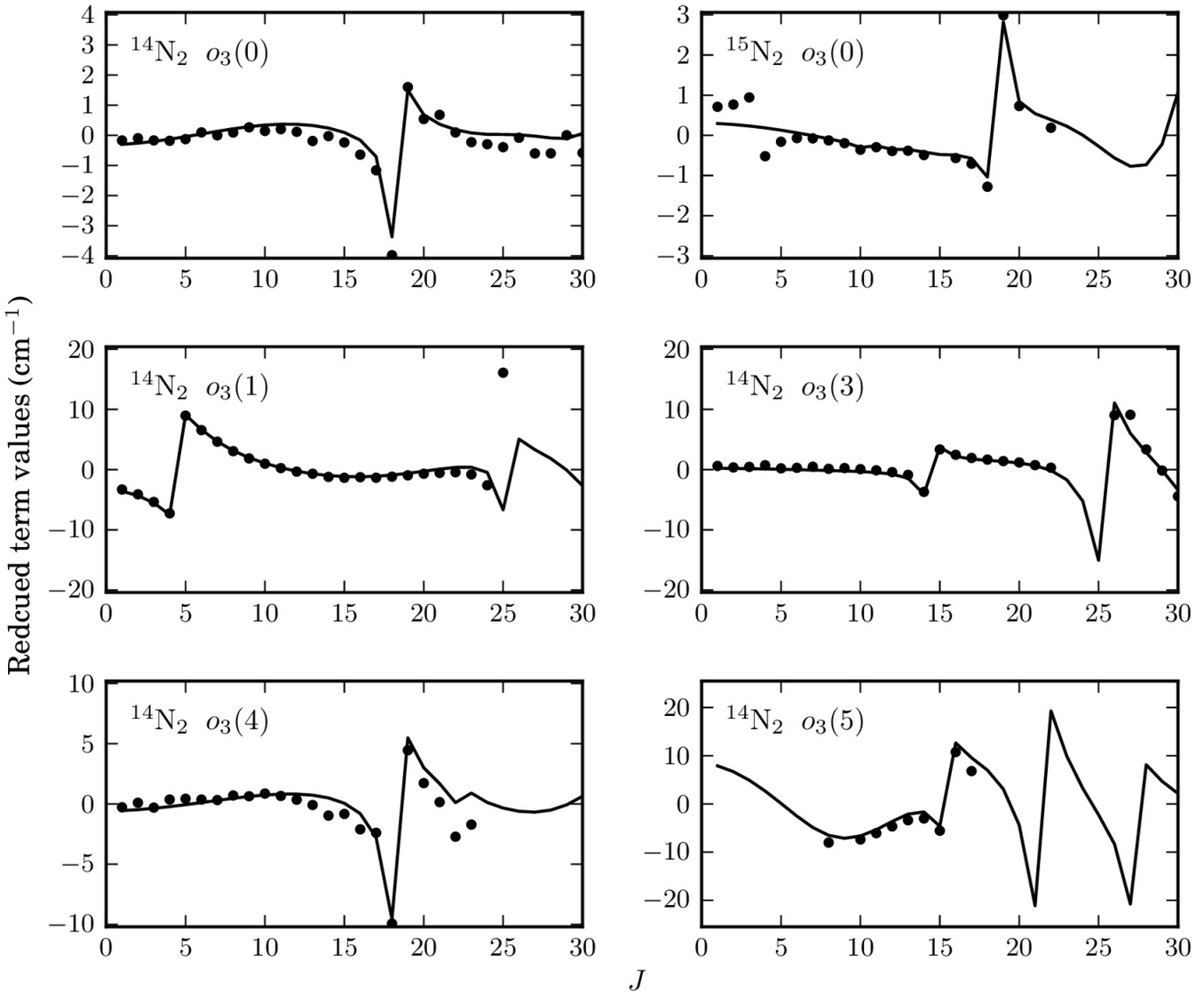

$$b'\,^1\Sigma_u^+ \sim o_3\,^1\Pi_u = -0.65 \pm 0.05\,\mathrm{cm}^{-1}$$

p-complex l-uncoupling: $3p\pi \sim 3p\sigma = 2.01 \pm 0.01\,\mathrm{cm}$

Experimental and modelled predissociation linewidth of $^1\Pi_u$ states

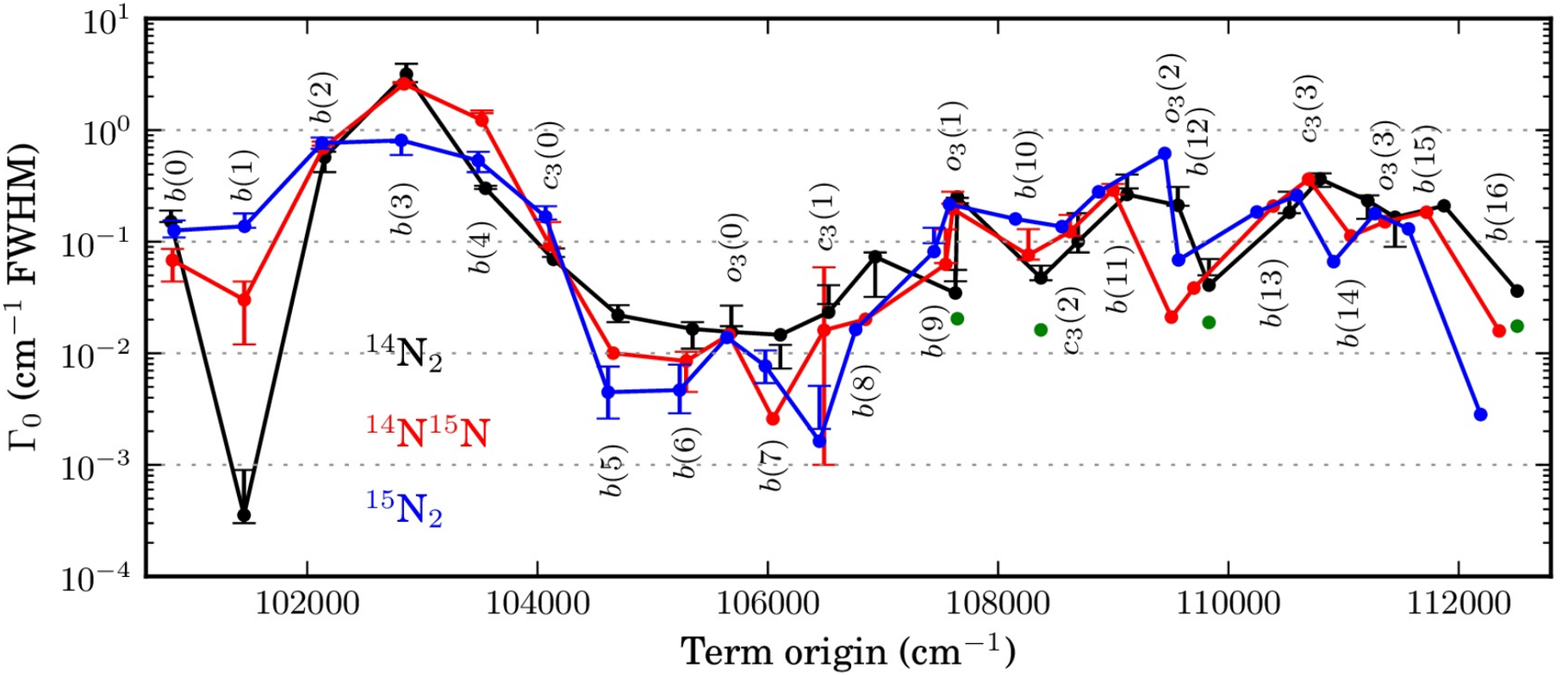

Direct observation of forbidden transitions with the SOLEIL FTS

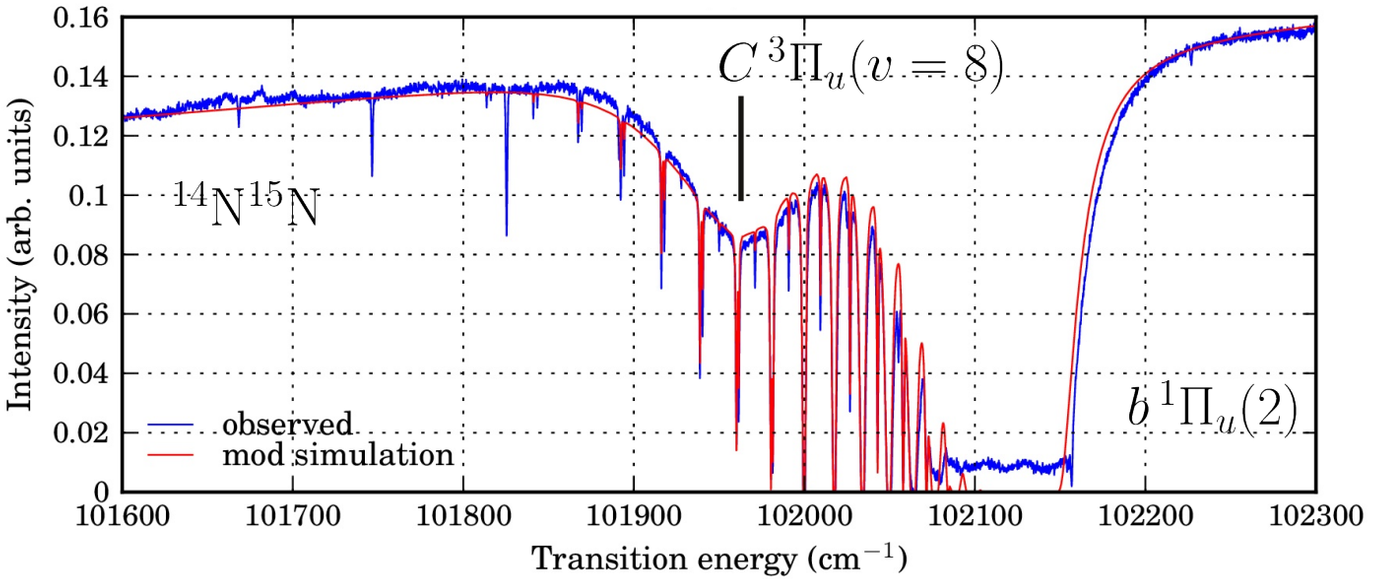

There is a feedback between modelling and experiment.

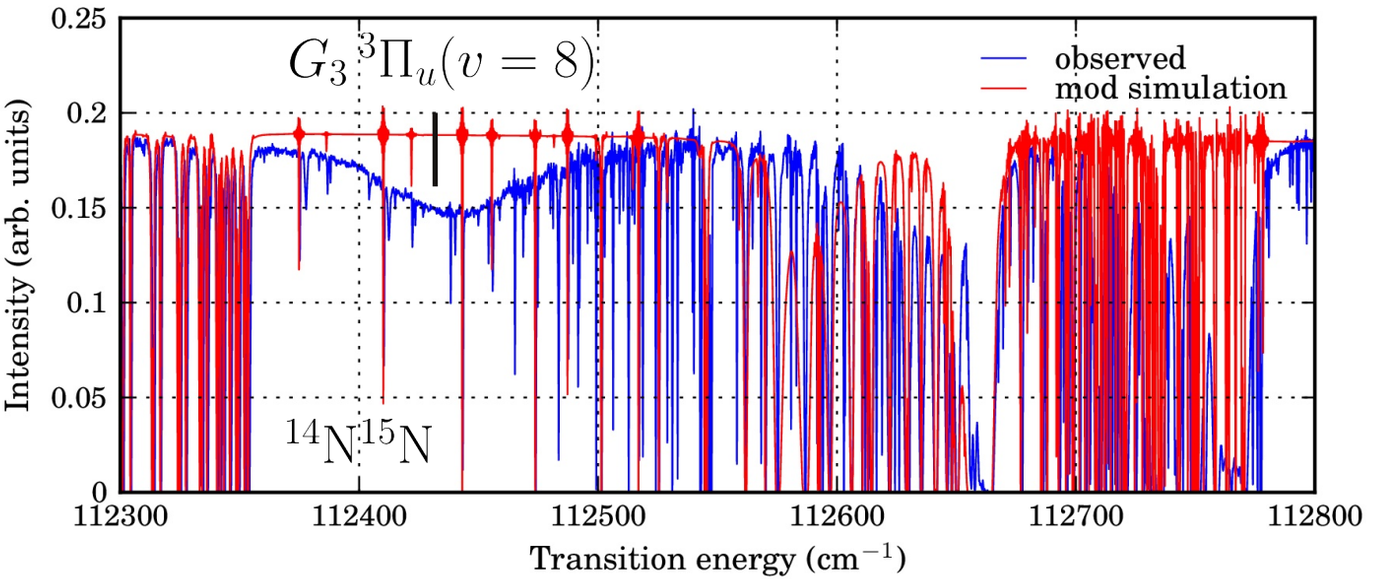

Summary

- Empirical aspects of this model are spectroscopically accurate.

- Quantum mechanical aspects are predictive.

- The methodology is convenient for exploring physical structure.

- Useful cross sections have been constructed.

- Builds upon *ab initio* calculations and laboratory measurements.

Lewis *et al.* (2005), *J. Chem. Phys.* 122:144302
Lewis *et al.* (2008), *J. Chem. Phys.* 129:164306
Heays *et al.* (2011), *J. Chem. Phys.* 135:244301
Heays *et al.* (2012), *Phys. Rev. A* 85:012705
Li, *et al.* (2013), *A&A*, accepted

TABLE III: Model matrix elements used in the CSE model (cm^{0-1}) as a function of J and R (Å). Fitting uncertainties are those calculated by the least squares optimisation routine.

Electronic interactions

$$\langle b\,^1\Pi_u|H^{\rm el}|c_3\,^1\Pi_u\rangle = (-1261 \pm 1) \times e^{-(R-0.906)^2/0.355}$$
$$\langle b\,^1\Pi_u|H^{\rm el}|c_4\,^1\Pi_u\rangle = (-166 \pm 1) \times e^{-(R-0.906)^2/0.355}$$
$$\langle b\,^1\Pi_u|H^{\rm el}|o_3\,^1\Pi_u\rangle = (368 \pm 1) \times e^{-(R-0.968)^2/0.276}$$
$$\langle c_3\,^1\Pi_u|H^{\rm el}|c_4\,^1\Pi_u\rangle = 0^a$$
$$\langle c_3\,^1\Pi_u|H^{\rm el}|o_3\,^1\Pi_u\rangle = (3149 \pm 1) \times e^{-(R-0.670)^2/0.383}$$
$$\langle c_4\,^1\Pi_u|H^{\rm el}|o_3\,^1\Pi_u\rangle = (414 \pm 1) \times e^{-(R-0.670)^2/0.383}$$

$$\langle b'\,^1\Sigma_u^+|H^{\rm el}|c_4'\,^1\Sigma_u^+\rangle = (-1730 \pm 1) \times e^{-(R-1.003)^2/0.258}$$
$$\langle b'\,^1\Sigma_u^+|H^{\rm el}|c_5'\,^1\Sigma_u^+\rangle = (-1066 \pm 1) \times e^{-(R-1.003)^2/0.258}$$
$$\langle c_4'\,^1\Sigma_u^+|H^{\rm el}|c_5'\,^1\Sigma_u^+\rangle = 0^a$$

$$\langle C\,^3\Pi_u|H^{\rm el}|C'\,^3\Pi_u\rangle = 789 \pm 13$$
$$\langle F_3\,^3\Pi_u|H^{\rm el}|C'\,^3\Pi_u\rangle = 302 \pm 56$$
$$\langle G_3\,^3\Pi_u|H^{\rm el}|C'\,^3\Pi_u\rangle = 1331 \pm 30$$
$$\langle F_3\,^3\Pi_u|H^{\rm el}|G_3\,^3\Pi_u\rangle = 1102 \pm 40$$

Rotational L-uncoupling[b]

$$\langle b\,^1\Pi_{u,e}|H^{\rm rot}|b'\,^1\Sigma_u^+\rangle = -B(R)\sqrt{J(J+1)} \cdot (-0.13 \pm 0.03)$$
$$\langle c_3\,^1\Pi_{u,e}|H^{\rm rot}|c_4'\,^1\Sigma_u^+\rangle = -B(R)\sqrt{J(J+1)} \cdot (2.01 \pm 0.01)$$
$$\langle c_4\,^1\Pi_{u,e}|H^{\rm rot}|c_5'\,^1\Sigma_u^+\rangle = -B(R)\sqrt{J(J+1)} \cdot (1.96 \pm 0.03)$$
$$\langle o_3\,^1\Pi_{u,e}|H^{\rm rot}|b'\,^1\Sigma_u^+\rangle = -B(R)\sqrt{J(J+1)} \cdot (-0.65 \pm 0.05)$$

Diagonal spin-orbit matrix elements[c]

$$\langle C\,^3\Pi_{u,\Omega=1}|H^{\rm SO}|C\,^3\Pi_{u,\Omega=2}\rangle = R\text{-dependent}^d$$
$$\langle C'\,^3\Pi_{u,\Omega=1}|H^{\rm SO}|C'\,^3\Pi_{u,\Omega=2}\rangle = 0^a$$
$$\langle F_3\,^3\Pi_{u,\Omega=1}|H^{\rm SO}|F_3\,^3\Pi_{u,\Omega=2}\rangle = -38^a$$
$$\langle G_3\,^3\Pi_{u,\Omega=1}|H^{\rm SO}|G_3\,^3\Pi_{u,\Omega=2}\rangle = 2^a$$

Off-diagonal spin-orbit interactions

$$\langle C'\,^3\Pi_{u,\Omega=1}|H^{\rm SO}|b\,^1\Pi_u\rangle = -2.0 \pm 0.2$$
$$\langle C\,^3\Pi_{u,\Omega=1}|H^{\rm SO}|b\,^1\Pi_u\rangle = 46 \pm 2$$
$$\langle F\,^3\Pi_{u,\Omega=1}|H^{\rm SO}|o\,^1\Pi_u\rangle = -38^a$$
$$\langle G\,^3\Pi_{u,\Omega=1}|H^{\rm SO}|c\,^1\Pi_u\rangle = -4.1 \pm 0.7$$
$$\langle 2\,^3\Sigma^+_{u,\Omega=1}|H^{\rm SO}|b\,^1\Pi_u\rangle = 11 \pm 1$$

Rotational S-uncoupling[b a e]

$$\langle {}^3\Pi_{u,\Omega=1}|H^{\rm rot}|{}^3\Pi_{u,\Omega=0}\rangle = -B(R)\sqrt{J(J+1)} \cdot \sqrt{2}$$
$$\langle {}^3\Pi_{u,\Omega=1}|H^{\rm rot}|{}^3\Pi_{u,\Omega=2}\rangle = -B(R)\sqrt{J(J+1)-2} \cdot \sqrt{2}$$
$$\langle {}^3\Pi_{u,\Omega=0}|H^{\rm rot}|{}^3\Pi_{u,\Omega=2}\rangle = 0$$

[a] An assumed value, discussed in the text.
[b] $B(R) = \frac{\hbar^2}{2\mu R^2}$.
[c] $\langle {}^3\Pi_{u,\Omega=0}|H^{\rm SO}|{}^3\Pi_{u,\Omega=0}\rangle = -\langle {}^3\Pi_{u,\Omega=2}|H^{\rm SO}|{}^3\Pi_{u,\Omega=2}\rangle$.
[d] R-dependence given in Ref. 51.
[e] See Ref. 63 p. 213.

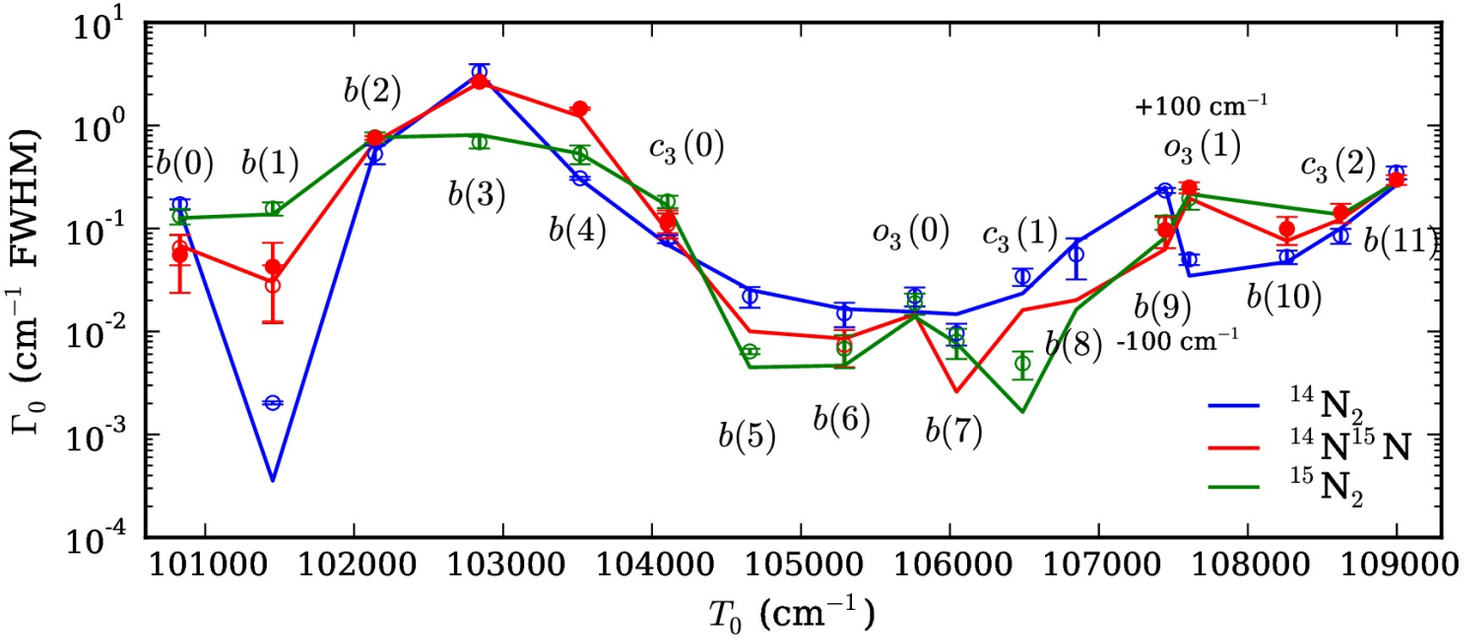
Γ_0 (cm^{-1} FWHM)
T_0 (cm^{-1})
$b(0)$ $b(1)$ $b(2)$ $b(3)$ $b(4)$ $b(5)$ $b(6)$ $b(7)$ $b(8)$ $b(9)$ $b(10)$ $b(11)$
$c_3(0)$ $c_3(1)$ $c_3(2)$
$o_3(0)$ $o_3(1)$
+100 cm^{-1}
-100 cm^{-1}
^{14}N$_2$
^{14}N^{15}N
^{15}N$_2$

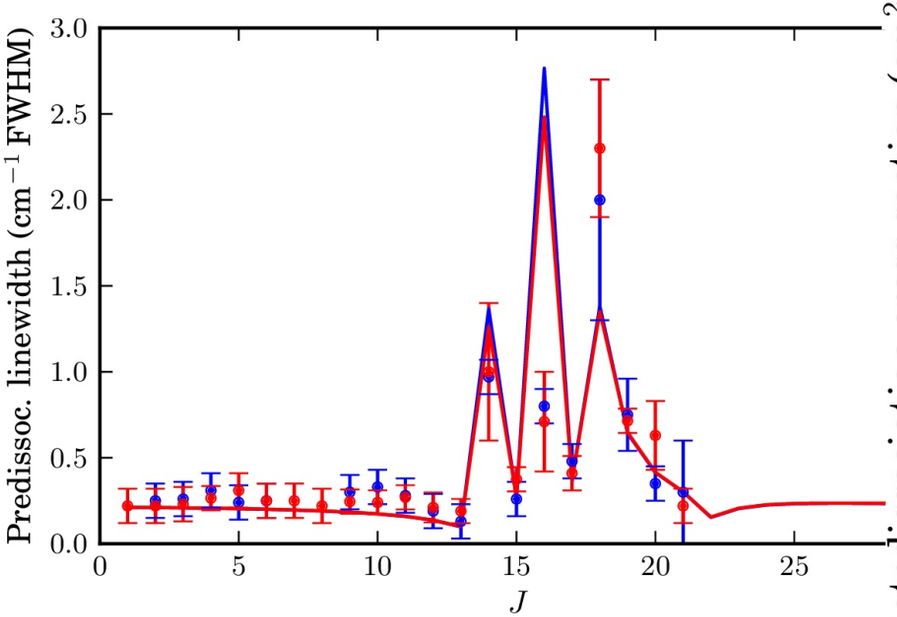
Predissoc. linewidth (cm^{-1} FWHM)
J

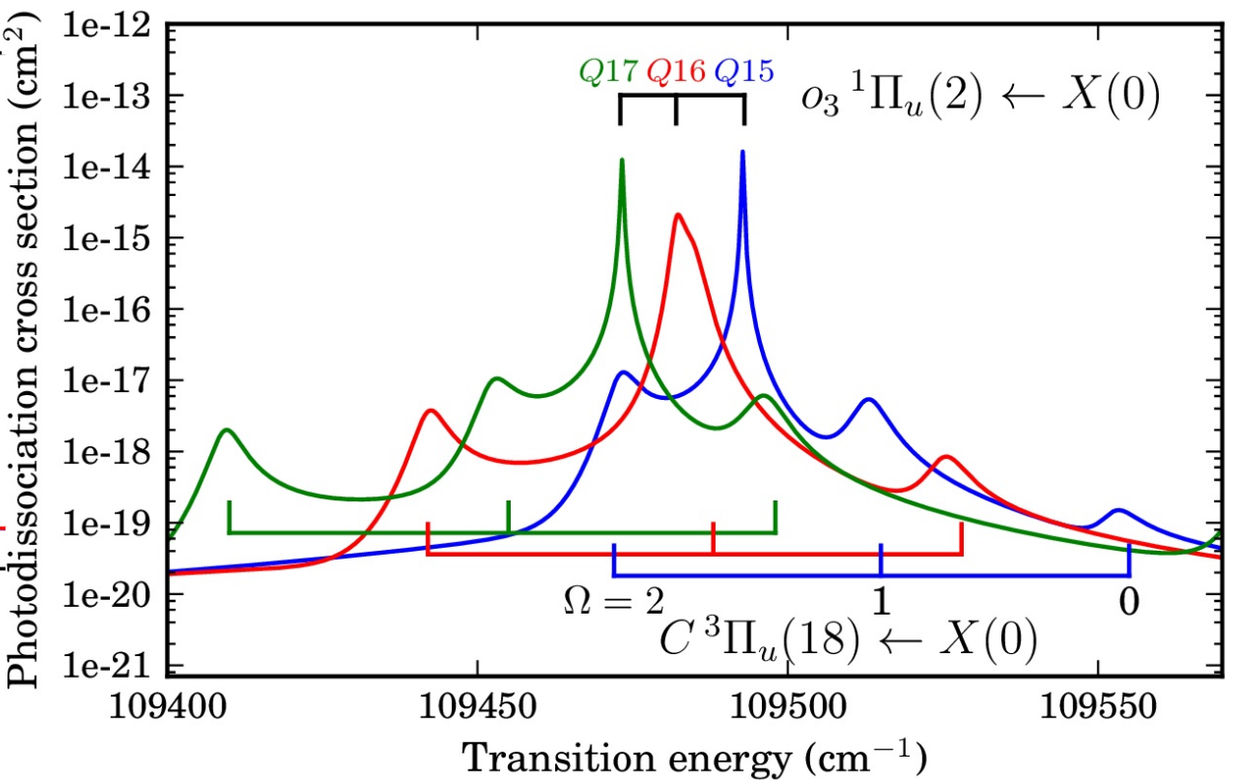
Photodissociation cross section (cm^2)
Transition energy (cm^{-1})
$Q17$ $Q16$ $Q15$
$o_3\,^1\Pi_u(2) \leftarrow X(0)$
$\Omega = 2$ 1 0
$C\,^3\Pi_u(18) \leftarrow X(0)$

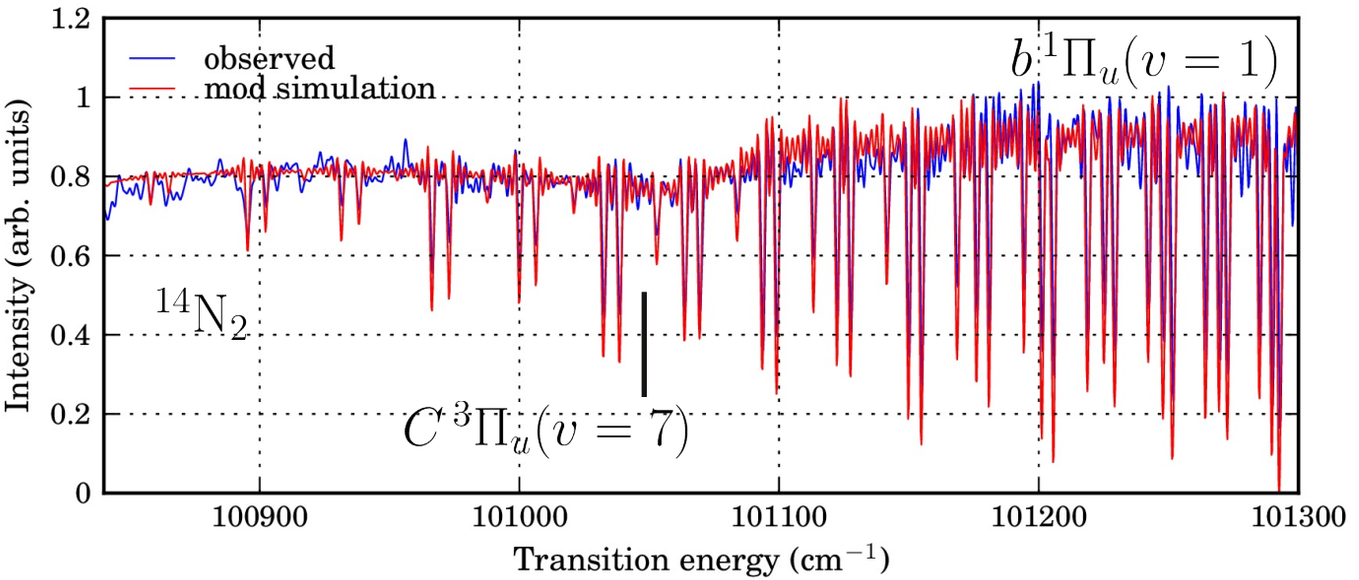
observed
mod simulation
$b\,^1\Pi_u(v=1)$
$^{14}N_2$
$C\,^3\Pi_u(v=7)$
Intensity (arb. units)
Transition energy (cm^{-1})
1.2
1
0.8
0.6
0.4
0.2
0
100900
101000
101100
101200
101300

Photodissociation

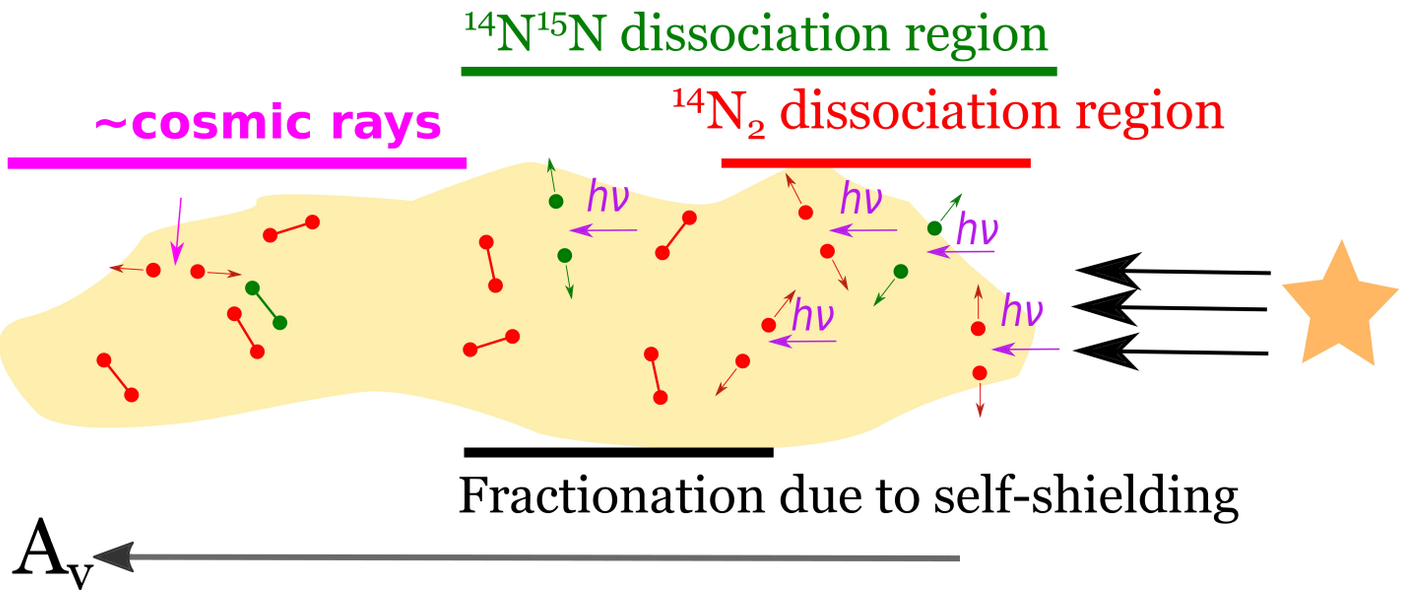

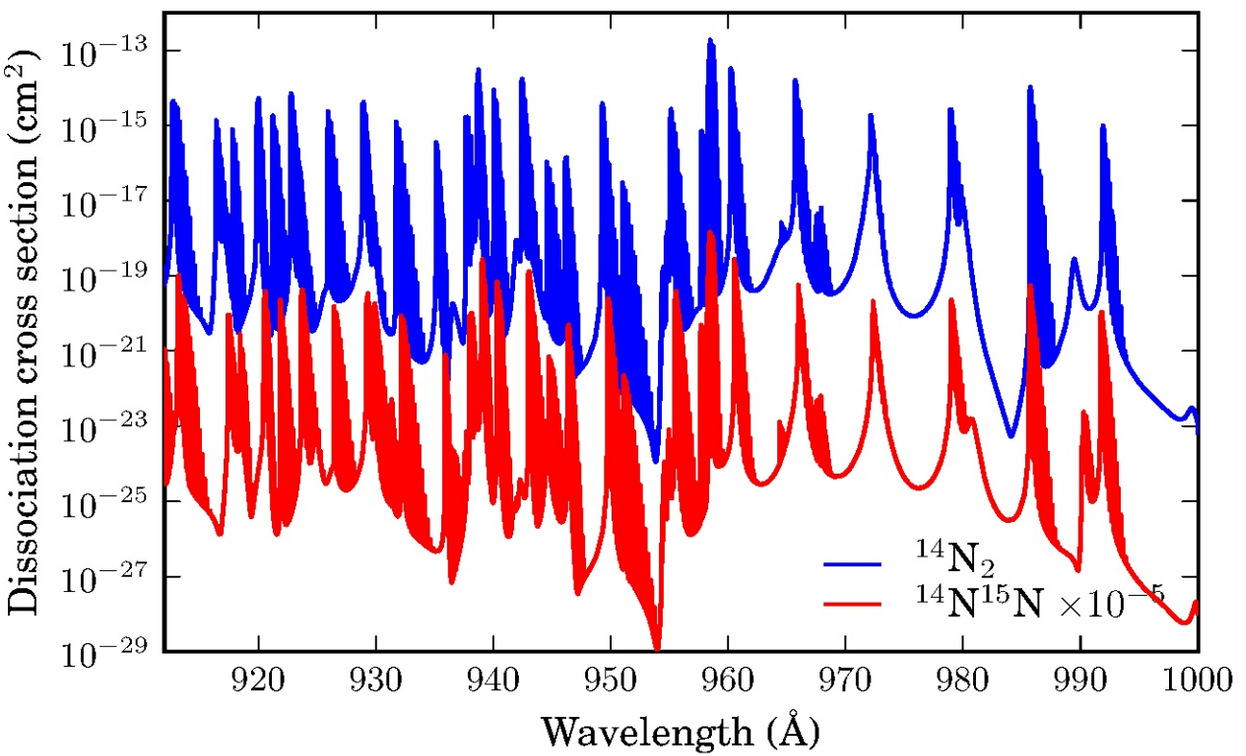

Photo-dissociation rate in a χ=1 Draine UV field

$^{14}N_2$ 30K : 1.66×10^{-10} s^{-1}
$^{14}N_2$ 1000K : 1.76×10^{-10} s^{-1}

$^{14}N^{15}N$ 30K : 1.70×10^{-10} s^{-1}
$^{14}N^{15}N$ 1000K : 1.85×10^{-10} s^{-1}

Isotopologue independent.

Shielding

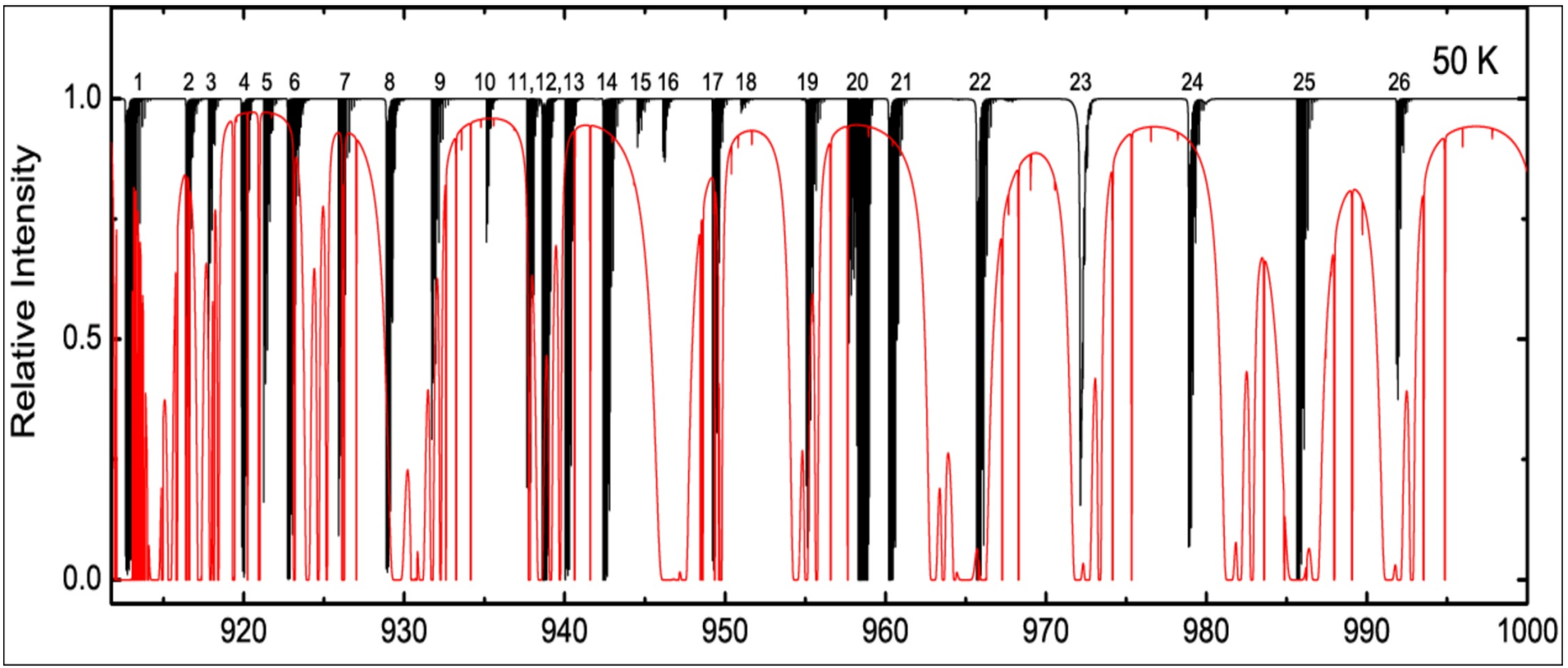

$N(H_2) = 1\times10^{20}$ cm^{-2} ⟼ 45% shielding
$N(H) = 5\times10^{20}$ cm^{-2}

$N(N_2) = 1\times10^{15}$ cm^{-2} ⟼ 65% shielding

Dust [given $N(H)$] ⟼ 20 - 80% shielding